

RSC Advances



This is an *Accepted Manuscript*, which has been through the Royal Society of Chemistry peer review process and has been accepted for publication.

Accepted Manuscripts are published online shortly after acceptance, before technical editing, formatting and proof reading. Using this free service, authors can make their results available to the community, in citable form, before we publish the edited article. This *Accepted Manuscript* will be replaced by the edited, formatted and paginated article as soon as this is available.

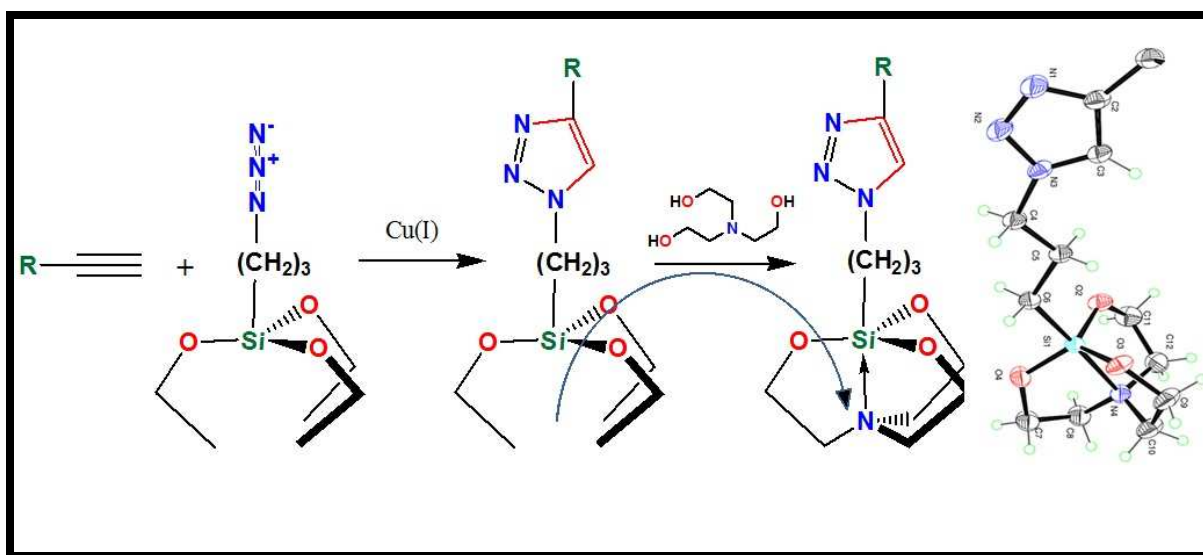
You can find more information about *Accepted Manuscripts* in the [Information for Authors](#).

Please note that technical editing may introduce minor changes to the text and/or graphics, which may alter content. The journal's standard [Terms & Conditions](#) and the [Ethical guidelines](#) still apply. In no event shall the Royal Society of Chemistry be held responsible for any errors or omissions in this *Accepted Manuscript* or any consequences arising from the use of any information it contains.

GRAPHICAL ABSTRACT

Design and Syntheses of Novel Fluorescent Organosilicon–Based Chemosensors Through

Click Silylation: Detection of Biogenic Amines

Gurjaspreet Singh^{a,*}, Satinderpal Singh Mangat^a, Hemant Sharma^b, Jandeep Singh^a, AanchalArora^a, Ajay Pal Singh Pannu^c, Narinder Singh^{b,*}

Synopsis: First report of the use of organosilicon–based chemosensors for the recognition of biogenic amines.

Design and Synthesis of Novel Fluorescent Organosilicon–Based Chemosensors Through Click Silylation: Detection of Biogenic Amines

Gurjaspreet Singh^{a,*}, Satinderpal Singh Mangat^a, Hemant Sharma^b, Jandeep Singh^a, Aanchal Arora^a, Ajay Pal Singh Pannu^c, Narinder Singh^{b,*}

^aDepartment of Chemistry and Centre of Advanced in Chemistry, Panjab University, Chandigarh, 160014, India

^bDepartment of Chemistry, Indian Institute of Technology, Ropar, 140001, Punjab, India

^cInstitute of Fundamental Sciences, Massey University, Private Bag 11 222, Palmerston North, New Zealand

*Corresponding authors: gjpsingh@pu.ac.in, nsingh@iitrpr.ac.in

ABSTRACT:

A concise and useful synthesis of novel 1,2,3-triazole based silatrane (TBS)–scaffolds (**2a–2e**) in good yield from 1,2,3-triazole based triethoxysilane (TBTES)–linkers (**1a–1e**) is described. Click silylation of terminal alkynes with γ -azidopropyltriethoxysilane (AzPTES) was used for the synthesis of TBTES–linkers (**1a–1e**). The synthesized TBS–scaffolds (**2a–2e**) were comprehensively characterized by ¹H and ¹³C NMR, mass spectrometry and single X-ray crystallographic studies. The broad scope of these TBS–scaffolds towards biogenic amines is explored by the use of CH₃CN:H₂O (98:2; v/v) solvent system. The receptor **2c** and **2d** shows high affinity towards spermine and histamine, respectively. To the best of our knowledge, the present investigation represents the first report of the use of organosilicon–based chemosensors for the recognition of biogenic amines.

INTRODUCTION

The term “Click Silylation” encompass the strategies of click and organosilicon chemistry that resulted into a powerful stratagem for the synthesis of 1,2,3-triazole based triethoxysilane (TBTES)–linkers; which are known for their immense biological and medicinal properties.¹⁻³ This research arena has received enormous attention owing to its aptitude to irreversibly couple two reactive molecular modules under ambient reaction conditions.⁴⁻¹¹ In order to augment the scope of TBTES–linkers, it is planned to modulate the precursor molecule for the synthesis of fluorogenic organosilicon based chemosensor (1,2,3-triazole based silatrane TBS–scaffolds). This approach has several advantages such as: a) it is a general method that can be readily extended to an extensive range of materials, including proteins, micelles, dye molecules and hybrid biomaterials;¹²⁻¹⁵ b) unlike TBTES–linkers, assembled TBS–scaffolds are stable to hydrolysis, oxidation and reduction; c) the ability of the N(3) atom of the 1,2,3-triazole and O(3) atom of silatrane ring to act as a hydrogen bond acceptor even makes it more attractive in supramolecular chemistry.

In continuation to our research motivation on sensor development for analytes of environmental and biological importance;¹⁶⁻²⁰ the present work is focused to develop sensor for biogenic amines, which are organic nitrogenous bases that regulate several physiological processes like body temperature, stomach pH, the immune response, brain activity, gastric acid secretion, cell growth and differentiation.²¹⁻²⁷ These amines may have endogenous origin (low concentration) or produced from microbial decarboxylation of amino acids (high concentration). A high content of these amines especially spermine, spermidine, putrescine and histamine caused intoxication in food; therefore level of these amines in food is a used as index of food quality.^{28,29} The estimation of spermine concentration in urine is an important parameter to check the

presence of tumors and monitor the effectiveness of cancer therapy.³⁰ Various methods are available for the detection of biogenic amines like gas chromatography,³¹ thin-layer LC (Liquid chromatography),^{32,33} reversed phase LC³⁴⁻³⁶ and LC with pre-column and post-column.³⁷⁻³⁹ Some of these techniques are extensively used due to low detection limit, high sensitivity and more accuracy.^{40,41} While huge setup, long estimation time and pretreatment of samples decreased the popularity of these methods. A chemosensors are better alternative for estimation of biogenic amines because they provide on-site detection, low detection limit and broad detection range. However, only few chemosensors have been reported so far and most of them are based on polymers, nanoparticles, hydrogel and polyelectrolytes.⁴²⁻⁴⁵ We herein report an interesting application of click silylation with the aim to assemble TBS-scaffolds, that may offers a number of imperative advantages as chemosensors. The interesting feature of this methodology is estimation of spermine level in the urine samples. For diagnosis and treatment of tumor, estimation of spermine in the urine is very helpful. Therefore, receptor **2c** was successfully utilized to detect the amount of spermine in the urine samples from tumor patients. The comparison of analytical parameters for general methods with present technique is as shown in Table 1.⁴⁶⁻⁴⁸ To the best of our knowledge, it is the first attempt to recognize the biogenic amine through organosilicon chemistry.

EXPERIMENTAL SECTION

Caution:

Azide compounds are explosive to heat and shock. Great care and protection are needed for heating of these compounds.

General material:

All the syntheses were carried out under dry nitrogen atmosphere using vacuum glass line. The organic solvents used were dried and purified according to the standard procedure⁴⁹ and stored under dry nitrogen atmosphere. Bromotris(triphenylphosphine)copper(I) (Aldrich), 3-chloropropyltriethoxysilane (Aldrich), propargyl alcohol (Aldrich), phenyl acetylene (Aldrich), triethanolamine (Merck), trisisopropanolamine (ALDRICH), propargyl bromide (Aldrich), sodium azide (SDFCL), morpholine (Fischer Scientific), phthalimide (ALDRICH), potassium hydroxide (SDFCL) were used as supplied. IR spectroscopic data was recorded on Thermo Scientific NICOLET iS50 FTIR instrument. ¹H and ¹³C NMR spectra were recorded on a Bruker Advance II 400 and JOEL 300 NMR spectrometer (in CDCl₃) at 25°C. Chemical shifts were reported in ppm relative to internal CDCl₃ and external tetramethylsilane (TMS). Mass spectral measurements (ESI source with capillary voltage, 2500V) were carried out on a VG Analytical (70-S) spectrometer. The compounds (3-azidopropyl)triethoxysilane, N-(propargyl)-morpholine, N-(propargyl)-phthalimide, 2-(prop-2-ynyl)oxybenzaldehyde used as a starting material in the present study were prepared according to published procedures^{1(a)}. The absorption spectra were measured on Specord 250 Plus Analytikjena spectrophotometer using quartz cells having 1 cm path length. The fluorescence spectra were recorded on a Perkin Elmer L55 spectrofluorimeter with scanning speed 400, excitation and emission slit width was 10 nm. The pH of solutions was recorded on Toschon pH meter.

Recognition studies

All studies were performed in CH₃CN/H₂O (98:2, v/v) solvent system. To get rid of kinetically errors, each spectrum is recorded after 15 min at 25°C. The selectivity of ligands was evaluated on UV-Visible and emission spectroscopy. The biogenic amine assay was performed in 5 mL volumetric flasks having 10 μM of ligand along with particular amine (histamine, spermine,

spermidine, tryamine, 1,2-Diaminopropane, 1,4-Diaminobutane, 1,5-Diaminopentane, 2-Phenylethylamine). For the selective amines, titrations were performed by successive addition of particular amine into solution of respective host (10 μM). The binding constant was calculated by Benesi-Hildebrand plot method and linear regression method was employed to determine the detection limit. The stoichiometry between amine and receptor was confirmed through Job's plot.⁵⁰ The maxima in the plot between $[\text{HG}]$ and $[\text{H}]/[\text{H}] + [\text{G}]$ correspond to stoichiometry of the complex.

X-Ray structure determination

X-ray data of TBS-scaffolds **2a**, **2b**, **2d** and **2e** were recorded at low temperature with a Rigaku-Spider X-ray diffractometer, comprising a Rigaku MM007 microfocus copper rotating-anode generator, high-flux Osmic monochromating and focusing multilayer mirror optics (Cu K radiation, $\lambda = 1.5418 \text{ \AA}$), and a curved image-plate detector. CrystalClear^{51(a)} was utilized for data collection and FSProcess in PROCESS-AUTO^{51(b)} for cell refinement and data reduction. The structures were solved by direct methods using SIR97^{51(c)} and refined by full-matrix least-squares refinement techniques on F2 using SHELXL-97^{51(d)} in the WINGX package^{51(e)} of programs. All non-hydrogen atoms were refined anisotropically. All other hydrogens were attached geometrically riding on their respective carrier atoms with Uiso being 1.5, 1.2, and 1.2 times the Uiso of their carrier methyl, methylene, and aromatic carbon atoms, respectively. The data measurement and other refinement parameters for these five crystal structures are given in Table 3.

Synthesis of compounds

Synthesis of 1-(3-(triethoxysilyl)propyl)-1H-1,2,3-triazol-4-yl)benzene (1a): A 50 mL two-neck round bottom flask was filled with phenyl acetylene (0.50 g, 4.90 mmol), AzPTES (1.21 g,

4.90 mmol), triethylamine (3.0 mL), and tetrahydrofuran (3.0 mL) under nitrogen atmosphere in the presence of [CuBr(PPh₃)₃] (cat. amount), and mixture was stirred at 60 °C for 5 h. The reaction mixture was allowed to cool, and then the solvents were removed under reduced pressure followed by addition of hexane and mixture was filtered. The filtrate was concentrated under reduced pressure to afford the title compound as brownish liquid in good yield Yield: 1.40 g, 83%. IR (neat): 2963, 2928, 2876, 1664, 1459, 1370, 1185, 965, 762 cm⁻¹. ¹H NMR (300 MHz, CDCl₃): δ_H = 7.77–7.64 (m, 3H), 7.24 (m, 3H), 4.29 (t, *J* = 7.0 Hz, 2H), 3.72 (q, *J* = 7.0 Hz, 6H), 2.09–1.83 (m, 2H), 1.14 (t, *J* = 7.0 Hz, 9H), 0.66–0.44 (m, 2H). ¹³C NMR (75 MHz, CDCl₃): δ_C = 130.6, 128.3, 127.5, 58.0, 53.3, 51.9, 23.9, 18.0, 7.2.

Synthesis of *N*-((1-(3-(triethoxysilyl)propyl)-1*H*-1,2,3-triazol-4-yl)methyl)phthalimide (*1b*):

This compound was synthesized following a similar procedure as for **1a**. However, *N*-(prop-2-ynyl)phthalimide (2.0 g, 10.81 mmol), AzPTES (2.67 g, 10.81 mmol), and [CuBr(PPh₃)₃] (cat. amount) were used here. Yield: 4.0 g, 85%. IR (neat): 2928, 2873, 1718, 1585, 1424, 1117, 908, 770 cm⁻¹. ¹H NMR (400 MHz, CDCl₃): δ_H = 7.77 (dd, *J* = 5.4, 3.1 Hz, 2H), 7.64 (dd, *J* = 5.5, 3.0 Hz, 2H), 7.54 (s, 1H), 4.91 (s, 2H), 4.24 (t, *J* = 7.2 Hz, 2H), 3.71 (q, *J* = 7.0 Hz, 6H), 1.95–1.88 (m, 2H), 1.12 (t, *J* = 7.0 Hz, 9H), 0.54–0.46 (m, 2H). ¹³C NMR (100 MHz, CDCl₃): δ_C = 166.5, 132.9, 130.9, 122.3, 121.8, 57.40, 51.37, 32.02, 23.14, 17.24, 6.48.

Synthesis of 2-((1-(3-(triethoxysilyl)propyl)-1*H*-1,2,3-triazol-4-yl)methoxy)benzaldehyde (*1c*):

This compound was synthesized following a similar procedure as for **1a**. However, 2-(prop-2-ynyloxy)benzaldehyde (1.0 g, 6.25 mmol), AzPTES (1.56 g, 6.31 mmol) and [CuBr(PPh₃)₃] (cat. amount) were used here. Yield: 1.50 g, 92%. IR (neat): 2922, 2872, 1680, 1599, 1454, 1285, 1190, 1055, 911, 939, 775, 702, 655, 584 cm⁻¹. ¹H NMR (300 MHz, CDCl₃): δ_H = 10.36 (s, 1H), 7.71 (d, *J* = 7.0 Hz, 2H), 7.46 (s, 1H), 7.14–6.93 (m, 2H), 5.25 (s, 2H), 4.31

(t, $J = 7.1$ Hz, 2H), 3.72 (q, $J = 8.6$ Hz, 6H), 1.99–1.95 (m, 2H), 1.13 (t, $J = 8.5$ Hz, 9H), 0.52–0.47 (m, 2H). ^{13}C NMR (75 MHz, CDCl_3): $\delta_{\text{C}} = 188.8, 160.4, 135.6, 128.5, 125.7, 121.0, 112.5, 62.4, 58.2, 52.2, 23.9, 18.1, 7.2$.

Synthesis of *N*–((1–(3–(triethoxysilyl)propyl)–1*H*–1,2,3–triazol–4–yl)methyl)morpholine (1d):

This compound was synthesized following a similar procedure as for **1a**. However, *N*–(propargyl)–morpholine (1.10 g, 4.45 mmol), AzPTES (0.56 g, 4.45 mmol) and $[\text{CuBr}(\text{PPh}_3)_3]$ (cat. amount) were used here. Yield: 1.57 g, 95%. IR (neat): 2958, 2927, 1454, 1285, 1073 cm^{-1} . ^1H NMR (400 MHz, CDCl_3): $\delta_{\text{H}} = 7.43$ (s, 1H), 4.28 (t, $J = 7.2$ Hz, 2H), 3.74 (q, $J = 7.0$ Hz, 6H), 3.65–3.61 (m, 4H), 3.59 (s, 2H), 2.47–2.41 (m, 4H), 1.99–1.91 (m, 2H), 1.15 (t, $J = 7.0$ Hz, 9H), 0.56–0.50 (m, 2H). ^{13}C NMR (100 MHz, CDCl_3): $\delta_{\text{C}} = 143.8, 132.08, 128.4, 122.5, 66.7, 58.47, 53.7, 53.4, 53.2, 24.1, 18.1, 7.4$.

Synthesis of (1–(3–(triethoxysilyl)propyl)–1*H*–1,2,3–triazol–4–yl)methanol (1e): This compound was synthesized following a similar procedure as for **1a**. However, propargyl alcohol (0.50 g, 8.92 mmol), AzPTES (2.20 g, 8.92 mmol) and $[\text{CuBr}(\text{PPh}_3)_3]$ (cat. amount) were used here. Yield: 2.50 g, 92%. IR (neat): 3364, 2930, 2875, 1460, 1309, 1271, 1080, 754 cm^{-1} . ^1H NMR (300 MHz, CDCl_3): $\delta_{\text{H}} = 7.46$ (s, 1H), 4.71 (s, 2H), 4.65 (s, 1H), 4.23 (t, $J = 6.9$ Hz, 2H), 3.72 (q, $J = 7.0$ Hz, 6H), 1.98–1.88 (m, 2H), 1.14 (t, $J = 7.0$ Hz, 9H), 0.52–0.47 (m, 2H). ^{13}C NMR (75 MHz, CDCl_3): 147.7, 121.8, 58.1, 55.6, 52.1, 23.8, 17.9, 7.1.

1–(3–(silatranyl)propyl)–1*H*–1,2,3–triazol–4–yl)benzene (2a): Compound **1a** (1.0 g, 2.86 mmol) and catalytic amount of potassium hydroxide was added to the stirred solution of triethanolamine (0.42 g, 2.86 mmol) in toluene (50.0 mL) in a 100.0 mL round–bottom flask fitted with a dean–stark apparatus. The reaction mixture was then refluxed at 110 °C for 5 h. The reaction mixture was brought to room temperature slowly in 1 h Toluene was removed under

vacuum and on slow addition of dry hexane (5.0 mL), clear white solid was precipitated out. The contents were further stirred for 1 hr at room temperature. The solid was filtered and washed twice with dry diethylether (2 x 5.0 mL) and dried under vacuum. The resulting solid was further dissolved in 20.0 mL of a 1:1 mixture of chloroform/ethanol and heated until a clear solution was obtained, which was then cooled slowly to room temperature and kept undisturbed for 5 days. White, thin shining needle like crystals in star shaped clusters suitable for single crystal X-ray analysis are isolated at room temperature. M.pt: 141 °C. Yield: 0.80 g, 78%. IR (neat): 2960, 2931, 2876, 1665, 1459, 1370, 1344, 1185, 1050, 965, 762, 692, 540 cm^{-1} . ^1H NMR (300 MHz, CDCl_3): $\delta_{\text{H}} = 7.78\text{--}7.74$ (m, 3H), 7.32–7.36 (m, 2H), 7.30 (s, 1H), 4.37 (t, $J = 5.8$ Hz, 2H), 3.77 (t, $J = 5.8$ Hz, 6H), 2.82 (t, $J = 5.8$ Hz, 6H), 2.00–2.06 (m, 2H), 0.61–0.36 (m, 2H). ^{13}C NMR (75 MHz, CDCl_3): $\delta_{\text{C}} = 128.7, 127.7, 125.6, 119.7, 55.6, 53.5, 50.9, 26.5, 13.3$. MS (ES+) calcd for $\text{C}_{17}\text{H}_{25}\text{N}_4\text{O}_3\text{Si}$ $[\text{M}+\text{H}]^+$ 361.2, found 361.2; Mass fragmentation (EI): 384 (13.7), 383 (65.5), 361 (100), 319 (11.9), 216 (3.9), 206 (7.7), 192 (8.4), 174 (27.7).

N-((1-(3-(silatranyl)propyl)-1H-1,2,3-triazol-4-yl)methyl)phthalimide (2b): This compound was synthesized following a similar procedure as for **2a**. However, triethanolamine (0.41 g, 2.78 mmol) and compound **1b** (1.20 g, 2.78 mmol) were used here. M.pt: 147 °C, Yield: 1.10 g, 89%, IR (neat): 2928, 2873, 1718, 1566, 1424, 1397, 1091, 908, 770, 712, 612, 578 cm^{-1} . ^1H NMR (400 MHz, CDCl_3): $\delta_{\text{H}} = 7.85$ (dd, $J = 5.4, 3.1$ Hz, 2H), 7.71 (dd, $J = 5.5, 3.0$ Hz, 2H), 7.62 (s, 1H), 4.98 (s, 2H), 4.27 (t, $J = 8.0$ Hz, 2H), 3.75 (t, $J = 5.8$ Hz, 6H), 2.81 (t, $J = 5.8$ Hz, 6H), 1.99–1.91 (m, 2H), 0.51–0.26 (m, 2H). ^{13}C NMR (100 MHz, CDCl_3): $\delta_{\text{C}} = 167.7, 142.2, 134.0, 132.1, 128.3, 123.4, 122.7, 59.1, 57.5, 53.4, 51.0, 33.2, 13.2$. MS (ES+) calcd for $\text{C}_{20}\text{H}_{26}\text{N}_5\text{O}_5\text{Si}$ $[\text{M}+\text{H}]^+$ 444.2, found 444.3; Mass fragmentation (EI): 482 (100), 483 (19.7), 462 (18.5), 444 (7.6), 402 (6.8), 279 (5.2), 192 (4.5), 174 (10.2), 150 (17.2), 132 (11.5).

2-((1-(3-(silatranyl)propyl)-1H-1,2,3-triazol-4-yl)methoxy)benzaldehyde 2c: This compound was synthesized following a similar procedure as for **2a**. However, Compound **1c** (1.0 g, 2.45 mmol) and triethanolamine (0.36 g, 2.45 mmol) were used here. M.pt.: 137 °C. Yield: 0.82 g, 78%. IR (neat): 2920, 2870, 1682, 1589, 1454, 1438, 1392, 1212, 1160, 1087, 1020, 939, 847, 775, 712, 702, 655, 584, 531 cm⁻¹. ¹H NMR (300 MHz, CDCl₃): δ_H = 10.41 (s, 1H), 7.76–6.97 (m, 5H), 5.25 (s, 2H), 4.28 (t, *J* = 6Hz, 2H), 3.68 (t, *J* = 3Hz, 6H), 2.74 (t, *J* = 3Hz, 6H), 1.97–1.88 (m, 2H), 0.37–0.32 (m, 2H). ¹³C NMR (75 MHz, CDCl₃): δ_C = 189.9, 160.8, 142.8, 136.0, 128.5, 122.8, 121.2, 113.2, 62.7, 57.5, 53.4, 50.9, 26.2, 13.0. MS (ES+) calcd for C₁₉H₂₇N₄O₅Si [M+H]⁺ 419.2, found 419.2; Mass fragmentation (EI): 459 (20.7), 458 (26.6), 457 (100), 441 (73.1), 419 (27.4), 297 (21.7), 215 (5.5), 192 (6.8), 174 (24.1), 172 (9.5), 150 (5.0). HRMS (ES⁺) calcd for C₁₉H₂₆N₄O₅Si [M+K]⁺ 457.1309, found 457.1317.

N-((1-(3-(silatranyl)propyl)-1H-1,2,3-triazol-4-yl)methyl)morpholine (2d): This compound was synthesized following a similar procedure as for **2a**. However, compound **1d** (1.61 g, 4.32 mmol) and triethanolamine (0.54 g, 3.60 mmol) were used here. M.pt: 124 °C, Yield: 1.23 g, 89%. IR (neat): 3336, 3121, 2941, 2879, 1597, 1453, 1324, 1265, 1085, 914, 758, 627, 576 cm⁻¹. ¹H NMR (400 MHz, CDCl₃): δ_H = 7.44 (s, 1H), 4.24 (t, *J* = 7.5 Hz, 2H), 3.70 (t, *J* = 4.2 Hz, 6H), 3.65–3.61 (m, 4H), 3.64 (s, 2H), 2.75 (t, *J* = 4.2 Hz, 6H), 2.54–2.41 (m, 4H), 2.01–1.96 (m, 2H), 0.43–0.39 (m, 2H). ¹³C NMR (100 MHz, CDCl₃): δ_C = 128.3, 121.6, 66.9, 59.4, 57.5, 57.0, 53.4, 51.0, 26.4, 13.2. MS (ES+) calcd for C₁₆H₃₀N₅O₄Si [M+H]⁺ 384.2, found 384.2; Mass fragmentation (EI): 423 (14.6), 422 (77.7), 385 (20.9), 384 (100), 174 (10.5), 172 (15.5), 150 (8.4), 132 (6.4).

(1-(3-(silatranyl)propyl)-1H-1,2,3-triazol-4-yl)methanol (2e): This compound was synthesized following a similar procedure as for **2a**. However, triethanolamine (0.47 g, 3.18

mmol) and compound **1e** (1.0 g, 3.18 mmol) was used here. M.pt: 143 °C, Yield: 1.0 g, 80%, IR (neat): 3364, 3137, 2930, 2875, 1439, 1351, 1271, 1080, 774, 670, 574 cm^{-1} . ^1H NMR (300 MHz, CDCl_3): δ_{H} = 7.50 (s, 1H), 4.70 (s, 2H), 4.26 (t, J = 7.5 Hz, 2H), 3.70 (t, J = 5.8 Hz, 6H), 2.75 (t, J = 5.8 Hz, 6H), 2.02–1.78 (m, 2H), 1.59 (s, 1H), 0.42–0.23 (m, 2H). ^{13}C NMR (75 MHz, CDCl_3): δ_{C} = 147.4, 121.5, 56.7, 55.3, 52.6, 50.1, 26.0, 13.0. MS (ES+) calcd for $\text{C}_{12}\text{H}_{23}\text{N}_4\text{O}_4\text{Si}$ $[\text{M}+\text{H}]^+$ 315.1, found 315.1; Mass fragmentation (ED): 315 (100), 337 (99.2), 338 (14.3), 273 (9.0), 216 (3.1), 192 (14.9), 174 (18.7), 150 (6.4).

RESULTS AND DISCUSSION

Structural aspects: The Scheme 1 illustrates the general synthetic route for the synthesis of TBS-scaffolds (**2a–2e**). Initially, azidopropyltriethoxysilane (AzPTES) was prepared by reacting sodium azide with 3-chloropropyltriethoxysilane in dry DMF at 90 °C for 4 h. For the Cu(I)-assisted click silylation of AzPTES, phenyl acetylene, N-(prop-2-ynyl)phthalimide, 2-(prop-2-ynyloxy)benzaldehyde, N-(propargyl)-morpholine and propargyl alcohol were selected as terminal alkynyl components. The reaction was performed in a very fruitful manner under $[\text{CuBr}(\text{PPh}_3)_3]$ -THF/ Et_3N system for the synthesis of TBTES-linkers (**1a–1e**). The IR spectrum reveals that the characteristic bands of the azido group ($-\text{N}=\text{N}=\text{N}$, 2091 cm^{-1}) and alkyne groups ($-\text{C}\equiv\text{C}$, 3279 and 2102 cm^{-1}) are no longer present after the click reaction. It is important to discuss here that ^1H NMR spectra of TBTES-linkers exhibit a triplet around $\delta \approx 1.14$ ppm and a quartet roughly at $\delta \approx 3.65$ ppm corresponding to CH_3 and OCH_2 of triethoxysilyl moiety, respectively. The downfield shift of triplet due to N_3CH_2 protons from $\delta = 3.19$ to $\delta \approx 4.19$ – 4.31 ppm signifies the C–N bond formation resulting into 1,2,3-triazole.

Finally, transesterification reaction in toluene was successfully carried out between TBTES-linkers (**1a–1e**) and triethanolamine in the presence of KOH at 110 °C for 5 h. All TBS-

scaffolds (**2a–2e**) (Table 2) were isolated as colorless crystalline solids that are insensitive to air and characterized by NMR (^1H and ^{13}C) and mass spectroscopy. In the ^1H NMR spectra of TBS–scaffolds shows two intense triplets characteristic feature of $\text{Si}(\text{OCH}_2\text{CH}_2)_3\text{N}$ moiety (due to protons of OCH_2 , $\delta \approx 3.75\text{--}3.78$ ppm and NCH_2 , $\delta \approx 2.80\text{--}2.83$ ppm) clearly distinguish silatranes from their parent compounds. In the ^{13}C NMR spectra, methylene carbon of propyl chain attached to silicon atom appears as the most shielded carbon atom, which is identified as $\delta \approx 12\text{--}13$ ppm. In the mass spectra of all compounds, $[\text{M} + \text{H}]^+$ peak appears with a very high intensity along with $[\text{M} + \text{Na}]^+$ and $[\text{M} + \text{K}]^+$ peaks. Fragmentation pattern of all TBS–scaffolds follows the general silatrane fragmentation as discussed in literature.⁵²

Crystals of compounds **2a**, **2b**, **2d** and **2e** for the X-ray experiment were grown from the saturated solutions in ethanol/ CHCl_3 . White, thin shining needle like crystals in star shaped clusters were isolated at room temperature. X-ray diffraction study has shown that compounds **2a**, **2b**, **2d** and **2e** were crystallized in a monoclinic crystal (Space group P 21/c), orthorhombic crystal system (Space group = Pbcu), triclinic crystal system (Space group = P-1) and monoclinic crystal system (Space group = C 2/c), respectively. The ORTEP view with atomic labelling (thermal ellipsoids were drawn at 50% probability) of compounds are shown in Figures 1A, 1B, 1C and 1D. X-ray crystal data and structure refinement details are listed in Table 3. Compounds of these types possess distorted trigonal bipyramidal geometry due to the presence of silatranyl skeleton. The most important parameter in silatranyl moiety was the Si-N bond length. This Si-N bond was clearly shorter than the sum of van der waals radii, which pointed out the weak bonding between both atoms. From the crystal data, it is clear that effect of 1,2,3-triazole moiety was not observed on the bond lengths of silatranyl moiety. It might be due to the presence of propyl chain between these moieties.

Fluorescence studies: Therefore by using click strategy, TBS-scaffolds (**2a–2e**) having binding groups directly attached to the 1,2,3–triazole ring have been synthesized in good yield and their affinity towards various biogenic amines were evaluated in CH₃CN:H₂O (98:2; v/v) solvent system. For this assay, eight different biogenic amines were employed and their structure are illustrate in Scheme 2. The interaction of biogenic amines with TBS-scaffolds (**2a–2e**) was evaluated in 5 mL volumetric flasks. As depicted in Figure S1A, the response of compound **2a** towards biogenic amines remains silent on fluorescence spectrophotometer. It did not represent any selectivity towards any particular biogenic amine. Similarly, the effect of biogenic amines on the emission properties of compound **2b** was evaluated and represented in Figure S1B. The compound **2b** also did not have any significant behavior towards any particular amines. Interestingly, it is observed that **2c** has high selectivity towards spermine (Figure 2A). The addition of 70 μ M of spermine leads to enhancement in fluorescence intensity at 393 nm. However, other biogenic amines did not produce any significant change in the emission profile of **2c** except spermine as shown in Figure 2B (excitation at 317 nm). The titration was performed to find out the mechanism behind this enhancement. The titration was accomplished in 10 mL volumetric flask having 10 μ M solution of **2c** along with stepwise addition of spermine (Figure 3A). From titration, the linear relationship was observed between fluorescence intensity at 393 nm and concentration of spermine in the range of 2 to 50 μ M (Figure 3B). To find out the stoichiometry of complex **2c**.spermine, a plot was drawn between [HG] and [H]/([H]+[G]) as shown in Figure S2A.⁵³ It has maxima at 0.6 which correspond to 2:1 stoichiometry between **2c** and spermine and has detection limit of 7 μ M. On analyzing of titration and job's plot of **2c**, it was hypothesized that a spermine molecule interacts with two molecules of **2c** through non-covalent interaction as shown in Scheme 3. These interactions produced change in the electronic

structure of the molecule and cancellation of PET channel, as a consequence of this enhancement in the intensity of **2c** was observed.⁵⁴ The effect of ionic strength was investigated by using tetrabutyl ammonium perchlorate (0–100 mM). It was observed that with the increase of ionic strength of the solution, emission profile of **2c** remain same as shown in Figure S2B. Further, to understand the role of medium pH on sensing behavior of **2c**, pH titrations were performed. The emission profile of **2c** unchanged in the pH range from 3 to 10 (Figure S3).

Inspired from these results and to extend its utility for practical purpose, **2c** was utilized for sensing of spermine in urine of tumor patient. Spermine is found in all eukaryotic cells and essential for cell growth and proliferation. The increase in content of spermine in urine may be indicative of tumor. Therefore, estimation of spermine in the urine of tumor patient is a good parameter to check the effectiveness of cancer treatment.^{55–57} Among various methods of detection, fluorescence spectroscopy is easiest and simplest technique for real time determination of spermine. To perform the assay, two patients who are under the treatment of Cholangiocarcinoma and Carcinoma Carcum from last two months are selected and their urine samples are collected randomly on a day. The urine samples are filtered through Whatman filter paper (4 μm) followed by centrifugation for 15 min at 400 rpm and whole process is repeated thrice. To standardize the procedure, different amounts (10 μl , 25 μl , 50 μl and 100 μl) of urine samples are added in 10 μM solution of **2c**. The enhancement in the intensity of **2c** is observed upon addition of urine samples and intensity has increased linearly with the amount of urine (10 μl to 100 μl) except control sample. In case of control sample, enhancement was observed once upon addition of 10 μl of urine; further addition did not cause any change. Therefore, standardized amount of urine sample (100 μl) was selected for analysis of spermine. The figure 4A revealed that addition of 100 μl of urine in the 5 mL of **2c** (10 μM) leads to enhancement in

fluorescence intensity, which is not so prominent in the control sample. These results increase the scope of this study as well as utility in real environment. Moreover, it is worth to elucidate the effect of other biogenic amines on the selectivity of receptor **2c** towards spermine. Therefore, a set of solutions were prepared having **2c** (10 μM) along with equal equivalent of spermine and other competing biogenic amines. As expected, the receptor **2c** has high selectivity even in the presence of other competing biogenic amines (Figure 4B).

In continuation, receptor **2d** and **2e** undergo a biogenic amine assay. The receptor **2d** gave a distinct response towards histamine among other amines and however, receptor **2e** does not show any particular response towards any amine (Figure S4). The addition of histamine (100 μM) to the solution of **2d** (10 μM) leads to new band at 376 nm (Figure 5A). To authenticate the binding, titration was performed between receptor **2d** and histamine in 10 mL volumetric flask (Figure 5B). The successive addition of histamine produced a smooth and linear enhancement in the fluorescence intensity at 376 nm. A calibration plot was drawn between fluorescence intensity and concentration of histamine and has linearity in the concentration range from (5–64 μM) as shown in Figure 6A. The detection limit has been calculated and it was about 5 μM . The job's plot was employed to reveal the stoichiometry of the complex **2d**.histamine. It has maxima at 0.5 which belong to 1:1 stoichiometry (Figure S5). The possible reason behind the arise of new band upon addition of histamine was ICT. The receptor **2d** has many electronegative groups and these groups form H-bonding with histamine molecule, which lead to charge transfer within in the molecule and new band was raised. Further, the selectivity of receptor **2d** towards histamine in the presence of other biogenic amines has been performed. The test was performed in 5 mL volumetric flasks, which contain receptor **2d** along with equal equivalent of histamine and other biogenic amines and placed for 2 h to attain the equilibrium. The Figure 6B clearly

illustrate the highly selective nature of receptor **2d** towards histamine in the presence other competing amines. The content of histamine has been used as index for the quality of food. During the storage of food article different preservatives have been employed. These preservatives have influence on the physiological environment of the cell. Therefore, it is essential to evaluate the effect of ionic strength and pH on the photophysical property of **2d**. It has been observed that ionic strength and pH has negligible effect on binding properties of receptor **2d** as shown in figure S6. For reproducibility, the relative standard deviation (RSD) of receptor **2c** (2.74 %) and receptor **2d** (3.01 %) has been calculated (n=4).

CONCLUSIONS

We have successfully demonstrated the use of click silylation for the synthesis of fluorogenic organosilicon based chemosensors (TBS-scaffolds) (**2a-2e**) from their corresponding TBTES-linkers (**1a-1e**). The scope of these TBS-scaffolds were extensively evaluated towards eight different biogenic amines and the receptors (**2c,2d**) proved their high affinity towards spermine and histamine respectively. The receptor **2c** efficiently detected the increased spermine level in the urine samples of the patients suffering from malignant tumors named Cholangio carcinoma and Carcinoma Carcum.

Acknowledgment

Authors are thankful to Dr. Paramvir Singh Mangat (PGIMER, Chandigarh) for collecting the urine samples of tumors patients.

REFERENCES

1. (a) Singh, G.; Mangat, S. S.; Singh, J.; Arora, A.; Sharma, R. K. *Tetrahedron Lett.* **2014**, 55, 903-909; (b) Burglov, K.; Moitra, N.; Hodacov, J.; Cattoen, X.; Man, M. W. C. *J. Org. Chem.* **2011**, 76, 7326–7333.

2. Cobos, O. D. L.; Fousseret, B.; Lejeune, M.; Rossignol, F.; Colas, M. D.; Carrion, C.; Boissiere, C.; Ribot, F.; Sanchez, C.; Cattoen, X.; Man, M. W. C.; Durand, J. O. *Chem. Mater.* **2012**, *24*, 4337–4342.
3. Moitra, N.; Moreau, J. J. E.; Cattoen, X.; Man, M. W. C. *Chem. Commun.* **2010**, *46*, 8416–8418.
4. Krasiński, A.; Fokin, V. V.; Sharpless, K. B. *Org. Lett.* **2004**, *6*, 1237–1240.
5. Kalisiak, J.; Sharpless, K. B.; Fokin, V. V. *Org. Lett.* **2008**, *10*, 3171–3174.
6. Morris, G. M.; Green, L. G.; Radić, Z.; Taylor, P.; Sharpless, K. B.; Olson, A. J.; Grynszpan, F. J. *Chem. Inf. Model.* **2013**, *53*, 898–906.
7. Grimster, N. P.; Stump, B.; Fotsing, J. R.; Weide, T.; Talley, T. T.; Yamauchi, J. G.; Nemečz, Á.; Kim, C.; Ho, K. -Y.; Sharpless, K. B.; Taylor, P.; Fokin, V. V. *J. Am. Chem. Soc.* **2012**, *134*, 6732–6740.
8. Millward, S. W.; Henning, R. K.; Kwong, G. A.; Pitram, S.; Agnew, H. D.; Deyle, K. M.; Nag, A.; Hein, J.; Lee, S. S.; Lim, J.; Pfeilsticker, J. A.; Sharpless, K. B.; Heath, J. R. *J. Am. Chem. Soc.* **2011**, *133*, 18280–18288.
9. Weide, T.; Saldanha, S. A.; Minond, D.; Spicer, T. P.; Fotsing, J. R.; Spaargaren, M.; Frère, J. M.; Bebrone, C.; Sharpless, K. B.; Hodder, P. S.; Fokin, V. V. *ACS Med. Chem. Lett.* **2010**, *1*, 150–154.
10. Valdez, C. A.; Tripp, J. C.; Miyamoto, Y.; Kalisiak, J.; Hruz, P.; Andersen, Y. S.; Brown, S. E.; Kangas, K.; Arzu, L. V.; Davids, B. J.; Gillin, F. D.; Upcroft, J. A.; Upcroft, P.; Fokin, V. V.; Smith, D. K.; Sharpless, K. B.; Eckmann, L. *J. Med. Chem.* **2009**, *52*, 4038–4053.

11. Dalvie, D. K.; Kalgutkar, A. S.; Khojasteh–Bakht, S. C.; Obach, R. S.; O'Donnell, J. P. *Chem. Res. Toxicol.* **2002**, *15*, 269–299.
12. Puri, J. K.; Singh, R.; Chahal, V. K. *Chem. Soc. Rev.* **2011**, *40*, 1791–1840.
13. (a) Holmes, R. R. *Chem. Rev.* **1990**, *90*, 17–31; (b) Holmes, R. R. *Chem. Rev.* **1996**, *96*, 927–950; (c) Corriu, R. J. P. *J. Organomet. Chem.* **1990**, *400*, 81–106; (d) Chuit, C.; Corriu, R. J. P.; Reye, C.; Young, J. C. *Chem. Rev.* **1993**, *93*, 1371–1448.
14. (a) Brennan, B. J.; Keirstead, A. E.; Liddell, P. A.; Vail, S. A.; Moore, T. A.; Moore, A. L.; Gust, D. *Nanotechnology* **2009**, *20*, 505203; (b) Frye, C. L.; Vogel, G. E.; Hall, J. A. *J. Am. Chem. Soc.* **1961**, *83*, 996–997.
15. Singh, R.; Puri, J. K.; Sharma, R. P.; Malik, A. K.; Ferretti, V. *J. Mol. Struct.* **2010**, *982*, 107–112.
16. Kaur, A.; Sharma, H.; Kaur, S.; Singh, N.; Kaur, N. *RSC Advances* **2013**, *3*, 6160–6166.
17. Fegade, U.; Sharma, H.; Attarde, S.; Singh, N.; Kuwar, A. *J. Fluoresc.* **2013**, 1–11.
18. Sharma, H.; Singh, A.; Kaur, N.; Singh, N. *ACS Sustainable Chemistry & Engineering* **2013**, *1*, 1600–1608.
19. Sharma, H.; Bhardwaj, V. K.; Kaur, N.; Singh, N.; Jang, D. O. *Tetrahedron Lett.* **2013**, *54*, 5967–5970.
20. Kim, M. J.; Sharma, H.; Singh, N.; Jang, D. O. *Inorg. Chem. Commun.* **2013**, *36*, 96–99.
21. Sharma, H.; Guadalupe, H. J.; Narayanan, J.; Hofeld, H.; Pandiyan, T.; Singh, N. *Analytical Methods* **2013**, *5*, 3880–3887.
22. Tabor, C.W.; Tabor, H. *Annu. Rev. Biochem.* **1984**, *53*, 749–790.
23. Cipolla, B. G.; Ziade, J.; Bansard, J. Y.; Moulinoux, J. P.; Staerman, F.; Quemener, V.; Lobel, B.; Guille, F. *Cancer* **1996**, *78*, 1055–1065.

24. Celano, P.; Baylin, S. B.; Casero, R. A. *J. Biol. Chem.* **1989**, *264*, 8922–8927.
25. Feuerstein, B. G.; Pattabiraman, N.; Marton, L. J. *Nucleic Acids Res.* **1990**, *18*, 1271–1282.
26. Brune, B.; Hartzell, P.; Nicotera, P.; Orrenius, S. *Exp. Cell Res.* **1991**, *195*, 323–329.
27. Khan, A. U.; Mei, Y. H.; Wilson, T. *Proc. Natl. Acad. Sci.* **1992**, *89*, 11426–11427.
28. Khan, U.; Mascio, P. D.; Medeiros, M. H. G.; Wilson, T. *Proc. Natl. Acad. Sci.* **1992**, *89*, 11428–11430.
29. Yang, X.; Rechnitz, G. A. *Electroanalysis* **1995**, *7* 105–108.
30. Kostereli, Z.; Severin, K., *Chemical Communications* **2012**, *48*, 5841-5843.
31. Staruszkiewicz, W.F.; Bond, J.F. *J. Assoc. Off. Anal. Chem.*, **1981**, *64* 584-591.
32. Nadeau, P.; Delaney, S.; Chouinard, L. *Plant Physiol.*, **1987**, *84*, 73-77.
33. Dibble, A.R.G.; Davies, P.J.; Mutscler, M.A. *Plant Physiol.*, **1988**, *86*, 338-340.
34. Reggiani, R.; Giussani, P.; Bertani, A. *Plant Cell Physiol.*, **1990**, *31*, 489-494.
35. Zambonin, P.G.; Guerrieri, A.; Rotunno, T.; Palmisano, F. *Anal. Chim. Acta*, **1991**, *251*, 101-107.
36. Oefner, P.J.; Wongyai, S.; Bonn, G. *Clin. Chim. Acta*, **1992**, *205*, 11-18.
37. Hauschild, M.Z. *J. Chromatogr.*, **1993**, *630*, 397-401.
38. Hyvonen, T.; Keinanen, T.A.; Khomutov, A.R.; Eloranta, T.O. *J. Chromatogr.*, **1992**, *574*, 17-21.
39. Ohta, H.; Takeda, Y.; Yoza, K.I.; Nogata, Y. *J. Chromatogr.*, **1993**, *628*, 199-215.
40. Tanima, D.; Imamura, Y.; Kawabata, T.; Tsubaki, K. *Org. Biomol. Chem.*, **2009**, *7*, 4689–4694.
41. Kielland, N.; Vendrell, M.; Lavilla, R.; Chang, Y-T. *Chem. Commun.*, **2012**, *48*, 7401–7403.

42. Yano, Y.; Yokoyama, K.; Tamiya, E.; Karube, I. *Anal. Chim. Acta.* **1996**, *320*, 269–276.
43. Kim, T. I.; Park, J.; Kim, Y. *Chem. Eur. J.* **2011**, *17*, 11978–11982.
44. Ikeda, M.; Yoshii, T.; Matsui, T.; Tanida, T.; Komatsu, H.; Hamachi, I. *J. Am. Chem. Soc.* **2011**, *133*, 1670–1673.
45. Lee, B.; Scopelliti, R.; Severin, K. *Chem. Commun.* **2011**, *47*, 9639–9641.
46. Cash, K. J.; Clark, H. A., *Analytical Chemistry* **2013**, *85*, 6312–6318.
47. Lange, J.; Wittmann, C., *Anal Bioanal Chem* **2002**, *372*, 276–283.
48. Plonka, J., *Analytical Methods* **2012**, *4*, 3071–3094.
49. Vogel, A. I. *A Text Book of Practical Organic Chemistry*, fourth ed., Longman, London, 1978.
50. Job, P. *Ann. Chim.* **1928**, *9*, 113–203.
51. (a) Rigaku, *CrystalClear. Version 1.4.0*, Rigaku Americas Corporation, The Woodlands, Texas, USA, 2005; (b) Rigaku, *PROCESS-AUTO*, Rigaku Corporation, Tokyo, Japan, 1998; (c) Sheldrick, G. M. *Acta Crystallogr.* **2008**, *A64*, 112–122; (d) Altomare, A.; Burla, M.C.; Camalli, M.; Cascarano, G. L.; Giacovazzo, C.; Guagliardi, A.; Moliterni, A. G. G.; Polidori, G.; Spagna, R. *J. Appl. Crystallogr.* **1999**, *32*, 115–119; (e) Sheldrick, G. M. *SHELXS-97. Program for the Solution of Crystal Structures*. University of Göttingen, Germany, 1997; (f) Farrugia, L. J. *J. Appl. Crystallogr.* **1999**, *32*, 837–838.
52. Puri, J. K.; Singh, R.; Chahal, V. K.; Sharma, R. P.; Wagler, J.; Kroke, E. *J. Organomet. Chem.* **2011**, *696*, 1341–1348.
53. Nakamura, M.; Sanji, T.; Tanaka, M. *Chem. Eur. J.* **2011**, *17*, 5344 – 5349.
54. Moinard, C.; Cynober, L.; Bant, J. P. *Clin. Nutr.* **2005**, *24*, 184–197.
55. Russel, D. H. *Clin. Chem.* **1977**, *23*, 22–27.

56. Wager, T. M. *J. Am. Chem. Soc.* **2007**, *129*, 16020–16028.

57. Russel, D. H. *Nature*, **1971**, *233*, 144–145.

Captions of Schemes, Figures and Tables:

Scheme 1. Synthesis of 1,2,3-triazole based silatrane (TBS)-scaffolds (**2a-2e**).

Scheme 2. Biogenic amines used in the present study.

Scheme 3: A mechanistic explanation of spermine binding with **2c**.

Figure 1A. Showing the ORTEP diagram with numbering Scheme for compound **2a** with 50% ellipsoidal probability.

Figure 1B. Showing the ORTEP diagram with numbering Scheme for compound **2b** with 50% ellipsoidal probability.

Figure 1C. Showing the ORTEP diagram with numbering Scheme for compound **2d** with 50% ellipsoidal probability.

Figure 1D. Showing the ORTEP diagram with numbering Scheme for compound **2e** with 50% ellipsoidal probability.

Figure 2: (A) Fluorescence spectra of **3** (10 μ M) upon addition of various biogenic amines (histamine, spermine, spermidine, tryamine, 1,2-Diaminopropane, 1,4-Diaminobutane, 1,5-Diaminopentane, 2-Phenylethylamine) in CH₃CN/H₂O (98:2; v/v) solvent system (excitation at 317 nm). (B) A change in fluorescence intensity at 393 nm in the presence various biogenic amines (histamine, spermine, spermidine, tryamine, 1,2-Diaminopropane, 1,4-Diaminobutane, 1,5-Diaminopentane, 2-Phenylethylamine).

Figure 3: (A) change in the emission profile of **2c** upon successive addition of spermine in CH₃CN/H₂O (98:2; v/v) solvent system (excitation at 317 nm); (B) The plot between fluorescence intensity at 393 nm and concentration of spermine. The linear relationship was observed in the concentration range of (0 to 50 μM).

Figure 4: (A) Fluorescence intensity of receptor **2c** in the urine of Cholangiocarcinoma, Carcinoma Carcum and healthy person (control) at 393 nm; (B) Effect of competing biogenic amines on the selectivity of receptor **2c** towards spermine.

Figure 5: (A) Fluorescence spectra of **2d** (10 μM) upon addition of various biogenic amines (histamine, spermine, spermidine, tryamine, 1,2-Diaminopropane, 1,4-Diaminobutane, 1,5-Diaminopentane, 2-Phenylethylamine) in CH₃CN/H₂O (98:2; v/v) solvent system (excitation at 270 nm); (B) change in the emission profile of **2d** upon successive addition of histamine in CH₃CN/H₂O (98:2; v/v) solvent system.

Figure 6: (A) The plot between fluorescence intensity at 376 nm and concentration of histamine. The linear relationship was observed in the concentration range of (5 to 64 μM); (B) Estimation of histamine through **2d** in the presence of other competing bioamines.

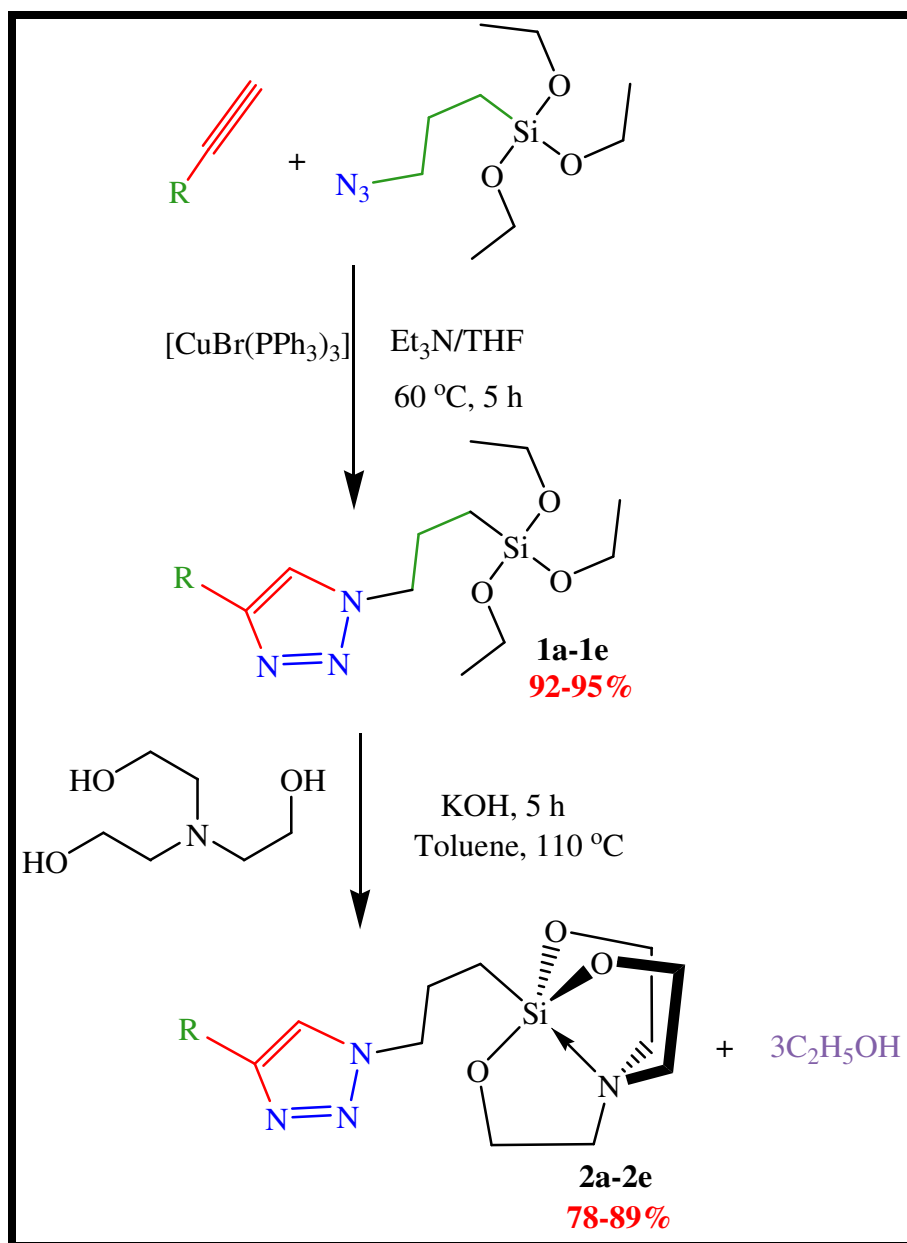
Table 1: A comparison of analytical parameters of present method with literature reported

Table 2: Synthesized 1,2,3-triazole based silatrane (TBS)-scaffolds (**2a-2e**).

Table 3: X-Ray Crystal Data and Structure Refinement for Compound **2a**, **2b**, **2d** and **2e**.

Table 1: A comparison of analytical parameters of present method with literature reported

Method	Limit of Detection	Sample Pretreatment	Analysis Time	Reproducibility
Enzyme Based Nanosensor ⁴⁶	1.1 mM for histamine	-	-	-
Enzyme Sensor Array ⁴⁷	10 mg/kg for histamine	Extraction and neutralization	3 min per sample	High, if using same electrode
HPLC ⁴⁸	0.5-2 mg/kg depending upon the amine	Extraction, neutralization, liquid-liquid extraction or solid phase extraction	30 min	Very high
Present Methodology	7 μ M for spermine, 5 μ M for histamine	Filtration and centrifugation	2 min	High



Scheme 1. Synthesis of 1,2,3-triazole based silatrane (TBS)-scaffolds (**2a-2e**).

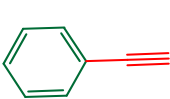
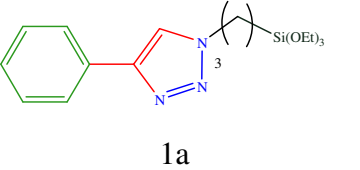
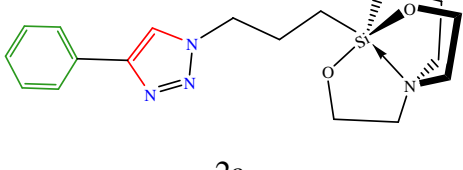
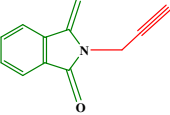
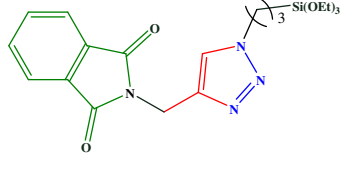
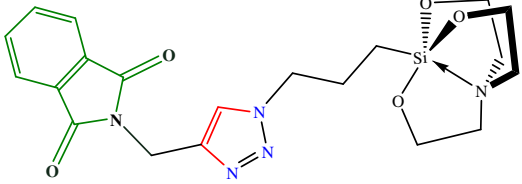
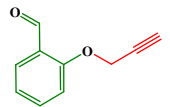
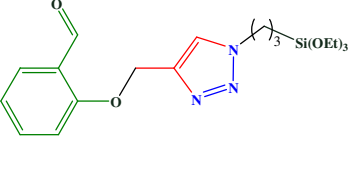
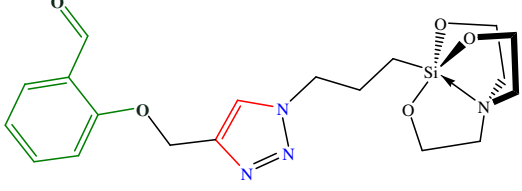
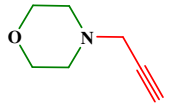
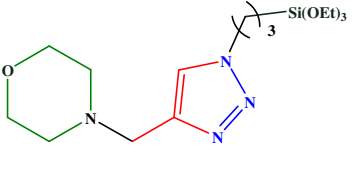
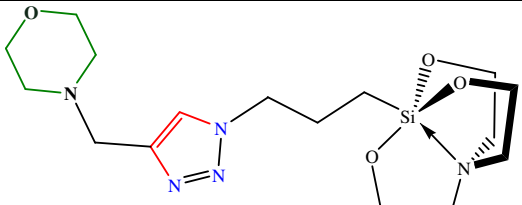

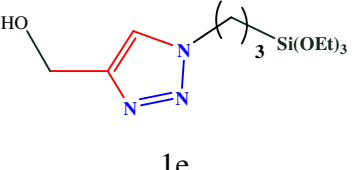
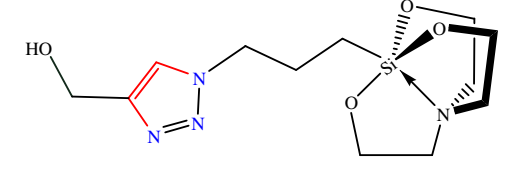
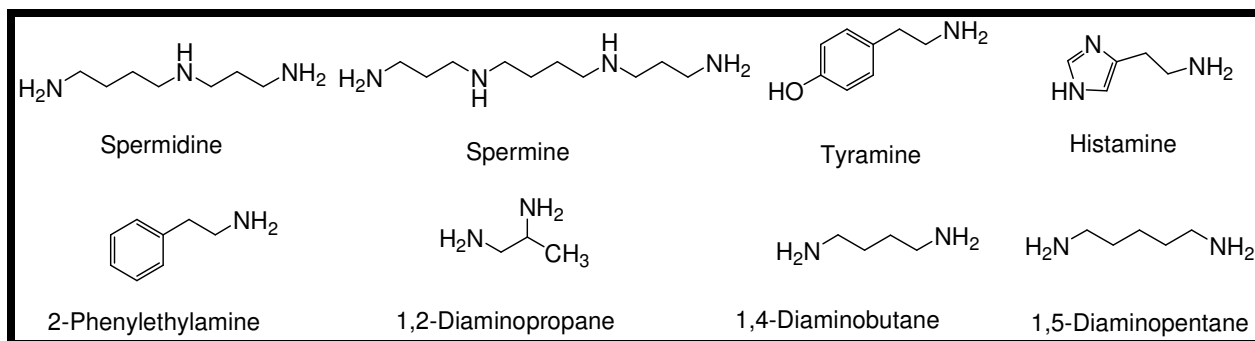
Terminal Alkynes (R—C≡C—)	TBTES-linkers (1a–1e)	Yield (%)	(TBS)-scaffolds (2a–2e)	Yield (%)
	 1a	92	 2a	78
	 1b	93	 2b	89
	 1c	93	 2c	78
	 1d	95	 2d	89
	 1e	92	 2e	80

Table 2: Synthesized 1,2,3-triazole based silatrane (TBS)-scaffolds (2a–2e).



Scheme 2. Biogenic amines used in the present study.

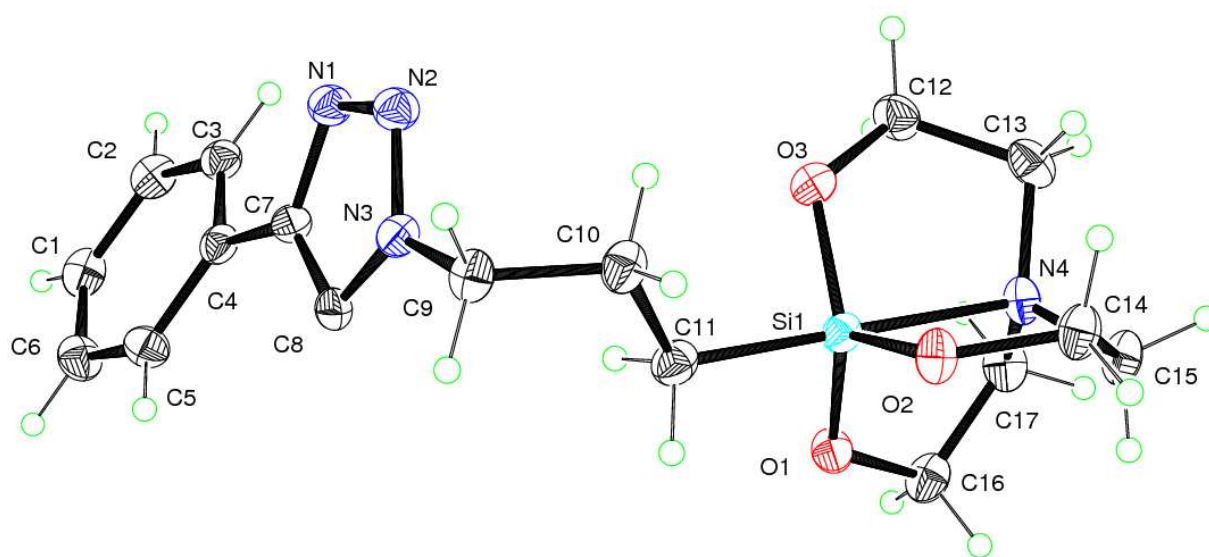


Figure 1A. Showing the ORTEP diagram with numbering Scheme for compound **2a** with 50% ellipsoidal probability.

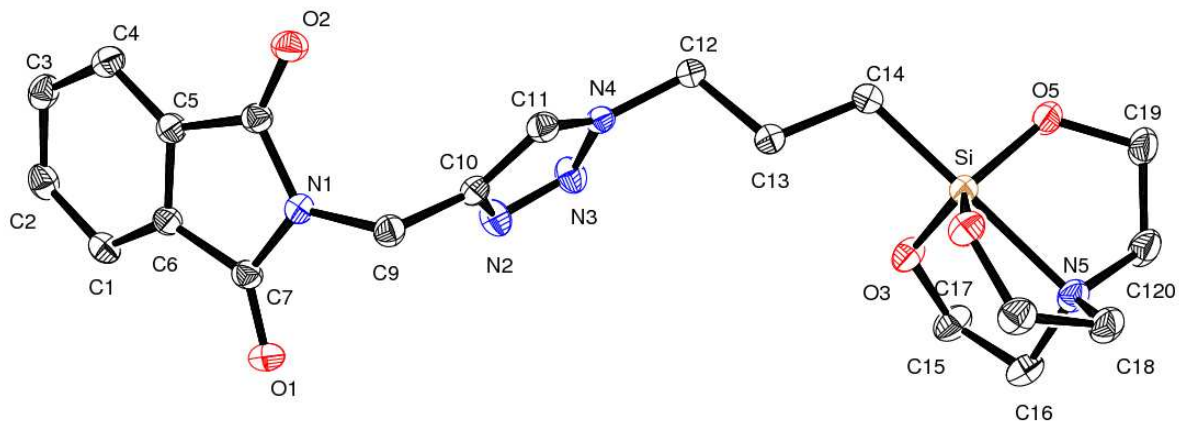


Figure 1B. Showing the ORTEP diagram with numbering Scheme for compound **2b** with 50% ellipsoidal probability.

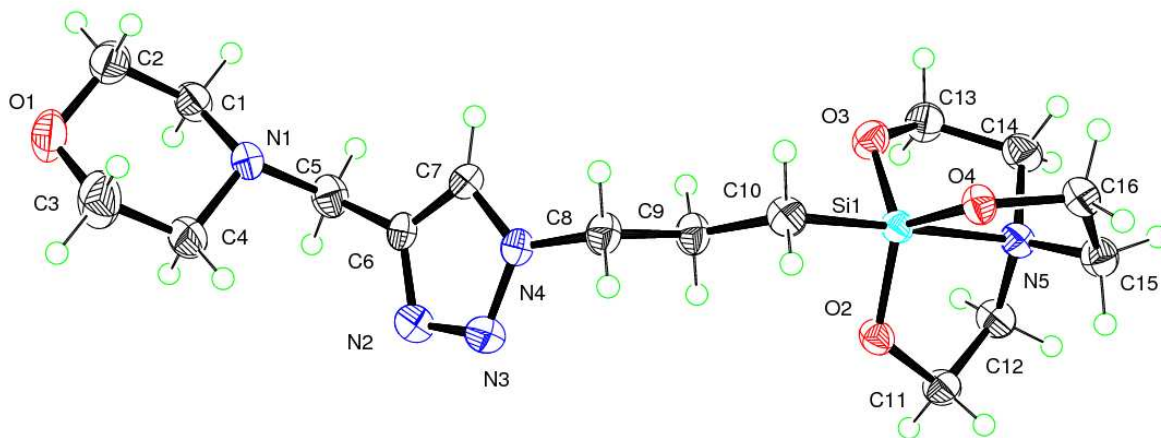


Figure 1C. Showing the ORTEP diagram with numbering Scheme for compound **2d** with 50% ellipsoidal probability.

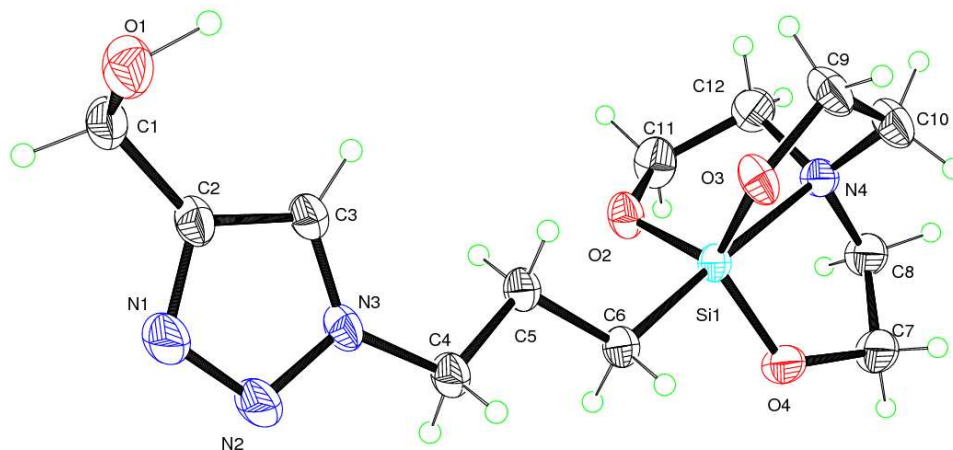


Figure 1D. Showing the ORTEP diagram with numbering Scheme for compound **2e** with 50% ellipsoidal probability.

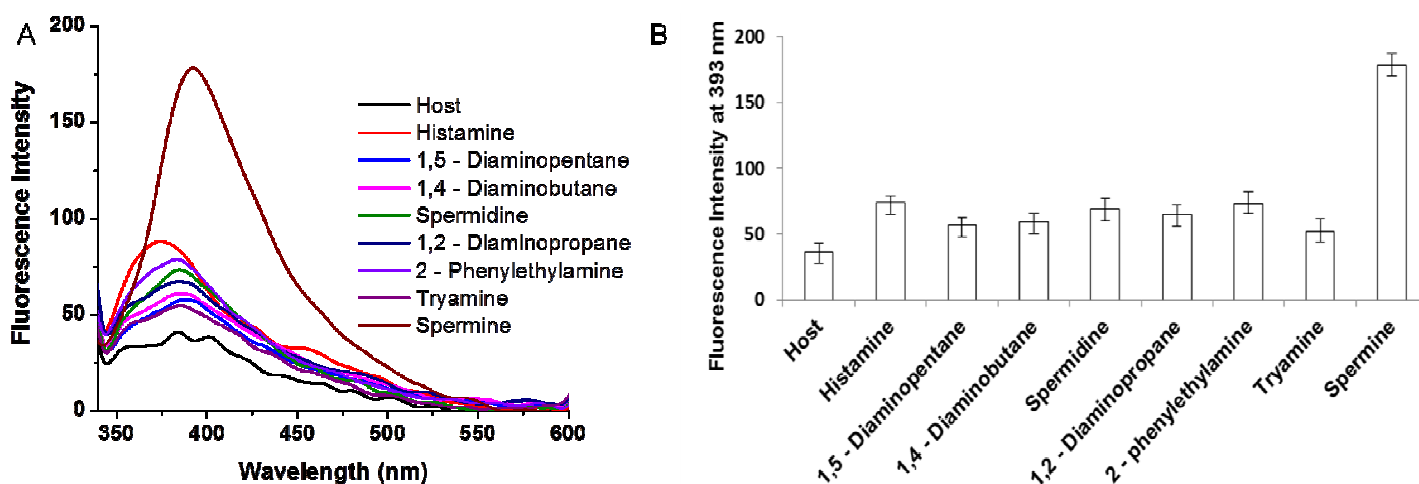
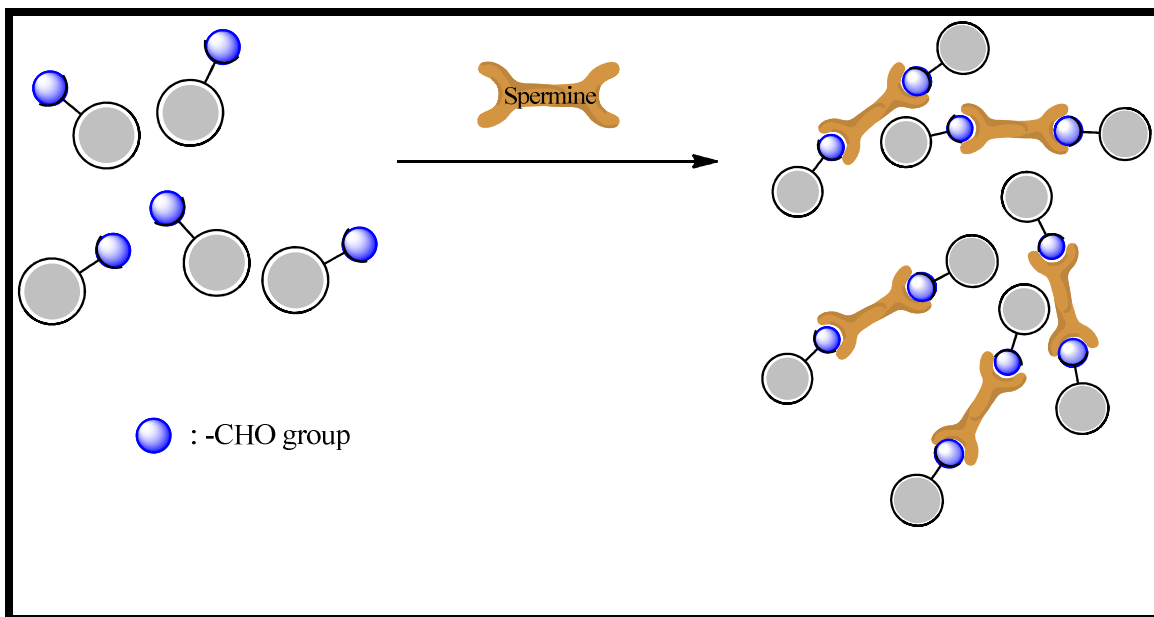


Figure 2: (A) Fluorescence spectra of **2c** (10 μ M) upon addition of various biogenic amines (histamine, spermine, spermidine, tryamine, 1,2-Diaminopropane, 1,4-Diaminobutane, 1,5-Diaminopentane, 2-Phenylethylamine) in $\text{CH}_3\text{CN}/\text{H}_2\text{O}$ (98:2; v/v) solvent system (excitation at 317 nm). (B) A change in fluorescence intensity at 393 nm in the presence various biogenic

amines (histamine, spermine, spermidine, tryamine, 1,2-Diaminopropane, 1,4-Diaminobutane, 1,5-Diaminopentane, 2-Phenylethylamine).



Scheme 3: A mechanistic explanation of spermine binding with 2c.

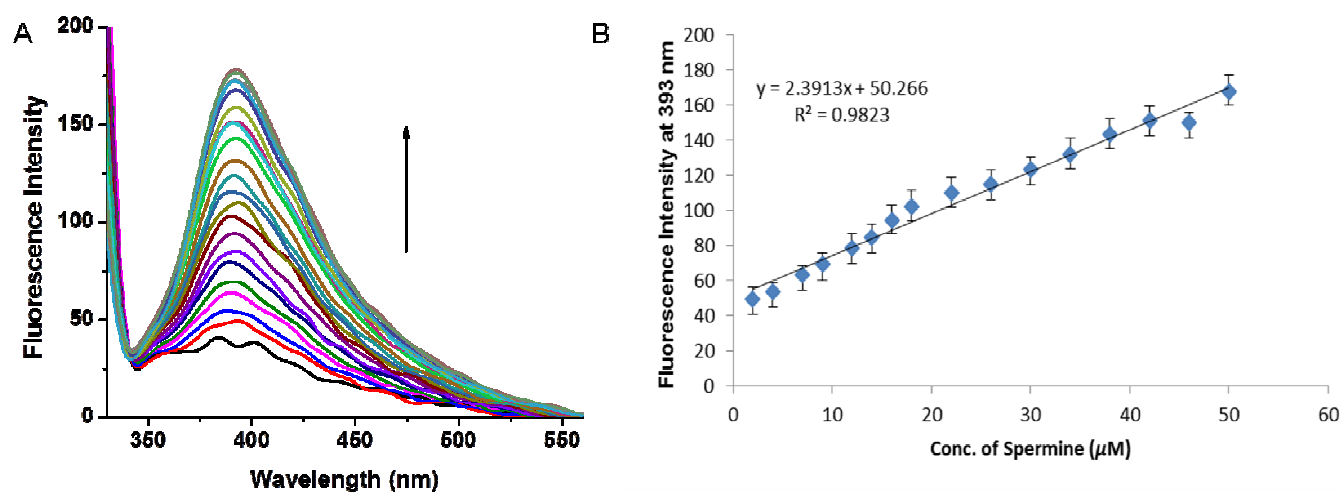


Figure 3: (A) change in the emission profile of **2c** upon successive addition of spermine in $\text{CH}_3\text{CN}/\text{H}_2\text{O}$ (98:2; v/v) solvent system (excitation at 317 nm); (B) The plot between fluorescence intensity at 393 nm and concentration of spermine. The linear relationship was observed in the concentration range of (0 to 50 μM).

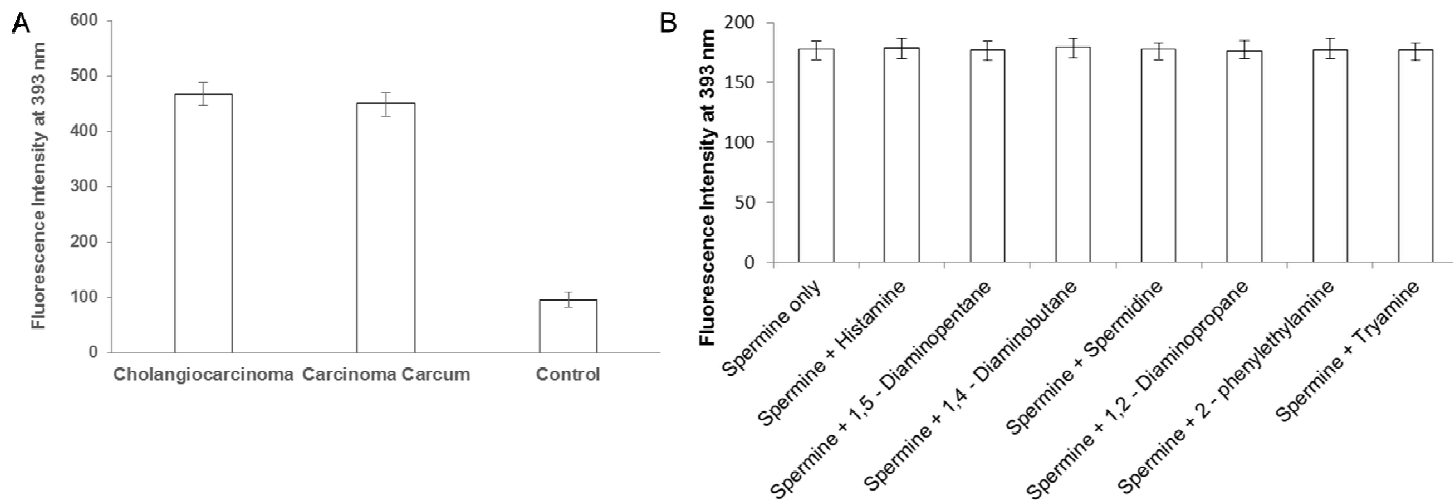


Figure 4: (A) Fluorescence intensity of receptor **2c** in the urine of Cholangiocarcinoma, Carcinoma Carcum and healthy person (control) at 393 nm; (B) Effect of competing biogenic amines on the selectivity of receptor **2c** towards spermine.

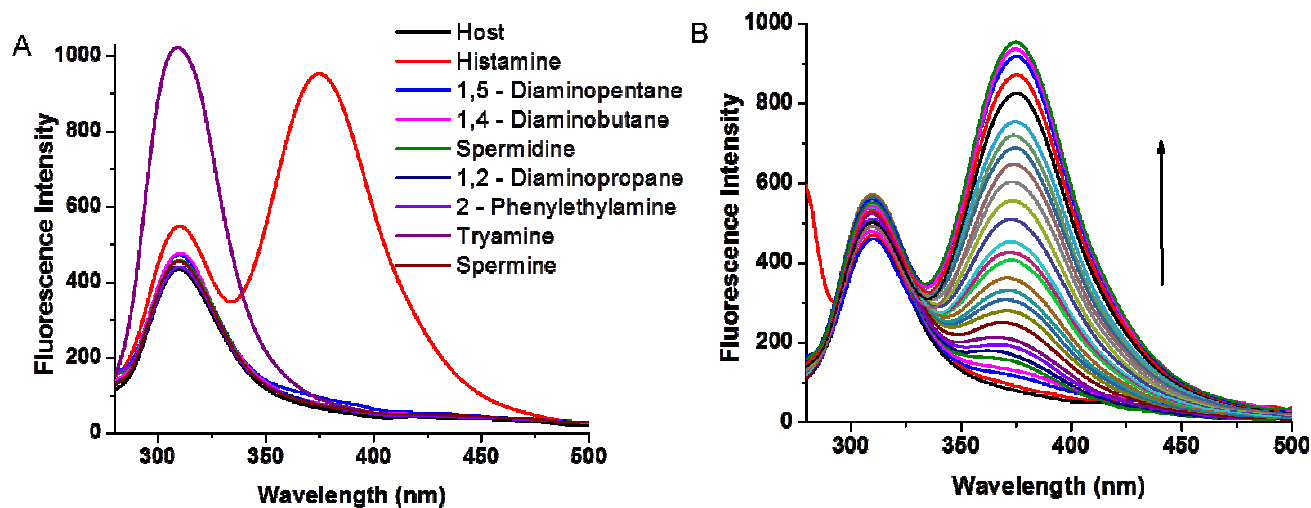


Figure 5: (A) Fluorescence spectra of **2d** (10 μM) upon addition of various biogenic amines (histamine, spermine, spermidine, tryamine, 1,2-Diaminopropane, 1,4-Diaminobutane, 1,5-Diaminopentane, 2-Phenylethylamine) in CH₃CN/H₂O (98:2; v/v) solvent system (excitation at

270 nm); (B) change in the emission profile of **2d** upon successive addition of histamine in CH₃CN/H₂O (98:2; v/v) solvent system.

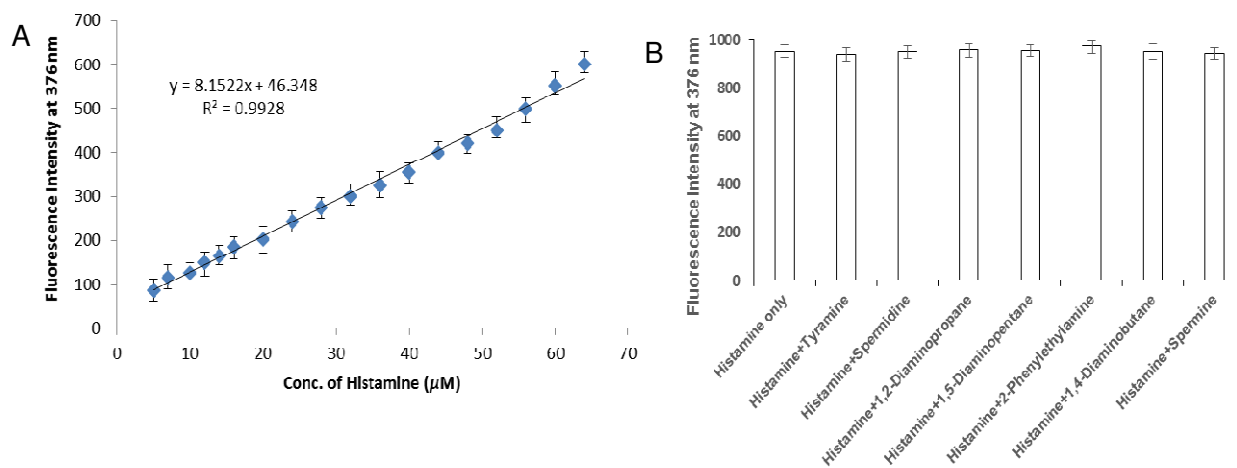


Figure 6: (A) The plot between fluorescence intensity at 376 nm and concentration of histamine. The linear relationship was observed in the concentration range of (5 to 64 μM); (B) Estimation of histamine through **2d** in the presence of other competing bioamines.

Table 3: X-Ray Crystal Data and Structure Refinement for Compound **2a**, **2b**, **2d** and **2e**.

Compound	2a	2b	2d	2e
Empirical formula	C ₁₇ H ₂₄ N ₄ O ₃ Si	C ₂₀ H ₂₅ N ₅ O ₅ Si	C ₁₆ H ₂₉ N ₅ O ₄ Si	C ₁₂ H ₂₂ N ₄ O ₄ Si
Formula weight	359.48	443.54	383.53	314.43
Temperature (K)	295(2)	295(2)	295(2)	295(2)
Wavelength(Å)	1.54178	1.54178	1.54178	1.54178
Crystal system,	Monoclinic	Orthorhombic	Triclinic	Monoclinic
Space group	P 21/c	P b c a	P -1	C 2/c
Unit cell dimensions				
a (Å)	11.151(5)	22.8796(5)	10.480(5)	23.2106(5)
b (Å)	18.583(5)	7.19450(10)	10.536(5)	11.4407(3)
c (Å)	8.759(5)	25.1019(18)	11.090(5)	14.1836(10)
α°	90	90	63.047(5)	90
β°	101.395(5)	90	73.639(5)	127.208(9)
γ°	90	90	65.682(5)	90
Volume (Å ³)	1779.3(14)	4132.0(3)	987.8(8)	2999.7(2)
Z	4	8	2	8
Calculated density (Mg/m ³)	1.342	1.426	1.289	1.392
Absorption coefficient	1.375	1.388	1.318	1.592

(mm ⁻¹)				
F(000)	764	1872	412	1344
Crystal size (mm)	0.20 x 0.18 x 0.18	0.20 x 0.18 x 0. 0.18	0.20 x 0.18 x 0.16	0.20 x 0.18 x 0.18
Theta range for data collection (°)	7.02 to 72.01	6.69 to 72.08	6.86 to 71.96	6.89 to 72.03
Max. and min. transmission	0.7899 and 0.7705	0.8084 and 0.7687	0.8168 and 0.7785	0.7625 and 0.7412
Refinement method	Full-matrix least-squares on F ²	Full-matrix least-squares on F ²	Full-matrix least-squares on F ²	Full-matrix least-squares on F ²
Data/restraints/parameters	3369 / 0 / 227	3981 / 0 / 280	3631 / 0 / 236	2878 / 0 / 194
Goodness-of-fit on F ²	1.666	1.150	1.204	1.124
R [I > 2s(I)]	R ₁ = 0.0519, wR ₂ = 0.1516	R ₁ = 0.0456, wR ₂ = 0.1277	R ₁ = 0.0454, wR ₂ = 0.1276	R ₁ = 0.0530, wR ₂ = 0.1484
R(all data)	R ₁ = 0.0609, wR ₂ = 0.1942	R ₁ = 0.0503, wR ₂ = 0.1295	R ₁ = 0.0534, wR ₂ = 0.1740	R ₁ = 0.0624, wR ₂ = 0.1701
Largest diff. peak and hole (e Å ⁻³)	0.763 and – 0.832	0.250 and – 0.361	0.527 and – 0.676	0.485 and – 0.433
CCDC no.	982459	982458	982460	982461